

Encapsulation of a copper(II) tetradentate Schiff base complex in zeolite NaY: an efficient heterogeneous catalyst for the synthesis of benzimidazoles

Akbar Mobinikhaledi · Mojgan Zendehtdel ·
Seyed Mohammad-Bagher Hosseini-Ghazvini ·
Parvin Safari

Received: 3 November 2014 / Accepted: 9 February 2015 / Published online: 24 February 2015
© Springer International Publishing Switzerland 2015

Abstract A copper(II) complex of 2,2'-(((methylenebis(oxy))bis(2,1-phenylene))-bis(azanylylidene))bis(methanylylidene)) diphenol (H₂L) was encapsulated in the supercages of zeolite NaY by the flexible ligand method. The resulting product was characterized by physicochemical and spectroscopic methods. The encapsulated complex and its corresponding free complex were used as catalysts for the synthesis of benzimidazoles. The results showed that the catalytic activity and stability of the complex were both increased by encapsulation. The effects of amount of catalyst, solvent, leaching and reusability of the heterogeneous catalyst were investigated.

Introduction

Imidazoles have a wide range of applications in pharmaceutical and chemical processes [1]. Significant biological activities including antiviral, anti-inflammatory, antidepressant, antitumor, antifungal, antimycotic, antibiotic, antiulcerative, antibacterial and anti-allergic [2] properties have been reported for imidazole derivatives. Furthermore, imidazoles find applications in green chemistry as ionic liquids and in N-heterocyclic carbenes [3].

The common methods for the synthesis of benzimidazole derivatives involve the condensation of carboxylic acids [4], acid chlorides [5], nitriles [6], orthoesters [7], amides [8],

esters [9] and aldehydes [10] with *o*-phenylene diamine over mineral acids such as H₂SO₄, HNO₃ and HF or Lewis acids such as AlCl₃ and BF₃ as catalysts. However, all of these procedures have some drawbacks such as low yields, utilization of expensive or hygroscopic reagents, high temperatures, special oxidation processes or long reaction times, tedious work-up procedures and side reactions. In order to avoid such problems, such conventional homogenous acid catalysts can be replaced with heterogeneous catalysts such as heteropolyacids, ion exchange resins (Amberlyst and Nafion-H), zeolites and clays. Advantages of such heterogeneous catalysts include low toxicity, availability and the possibility of reuse [11]. Among the various solid acid catalysts, zeolites have received increasing attention because of their suitable acidities, thermal stability, reusability and availability [12]. In connection of our previous work on the synthesis of benzimidazole derivatives using zeolite NaY as a catalyst [13], we wished to increase the yield and decrease the reaction time for the synthesis of benzimidazoles by encapsulating a new Schiff base complex in the supercages of zeolite NaY. The results of our experiments are reported in this paper.

Experimental

Materials and measurements

All materials and solvents were obtained from commercial sources (Merck or Fluka) and used as received. Zeolite NaY was prepared according to the method reported in the literature [14]. An X-ray diffractometer type XPERT with Cu-K_α radiation at room temperature was used for recording XRD patterns. Infrared spectra were recorded as KBr pellets on a Galaxy series FTIR 5000 spectrometer, in the range of

A. Mobinikhaledi · M. Zendehtdel ·
S. M.-B. Hosseini-Ghazvini (✉) · P. Safari (✉)
Department of Chemistry, Faculty of Science, Arak University,
38156-8-8349 Arāk, Iran
e-mail: smbhgh@yahoo.com

P. Safari
e-mail: P.Safary@gmail.com

500–4000 cm^{-1} . Also, a TG/DTA (Perkin-Elmer TG/DT 6300 thermo gravimetric analyzer), a BET apparatus (SIBATA, App. 1100-SA with adsorption of nitrogen at 77°K), a V-670 JASCO spectrophotometer and Elemental analyzer (Vario E1 III) were applied for characterization of the encapsulated complex. Finally, metal contents were measured using a 990 atomic absorption spectrophotometer provided by PG Instruments Ltd.

Preparation of the Schiff base

The Schiff base and its corresponding free complex were synthesized as reported previously [15]. Preparation of the Schiff base was performed according to the three following steps (as shown in Scheme 1).

Preparation of bis(2-nitrophenoxy)methane

A mixture of 2-nitrophenol (10 mmol) and dry K_2CO_3 (5 mmol) was dissolved in DMF (5 ml). The solution was added dropwise to a solution of 1,1-diiodomethane (5 mmol) in dry DMF (5 ml) and the reaction mixture was refluxed at 110–120 °C for 6 h. The mixture was then cooled and poured onto crushed ice. The precipitate was separated by filtration and washed with ethanol to produce the product (**1a**). Yield 68 %.

Preparation of 1,1-bis(2-aminophenoxy)methane

A mixture of **1a** (2 g), Pd/C 10 % (0.05 g) and hydrazine monohydrate 80 % (3 ml) was added to absolute ethanol (10 ml) and the mixture was refluxed for 5 h. After completion of the reaction, the mixture was filtered to remove Pd/C and then cooled to room temperature to give a precipitate, which was filtered off and recrystallized from ethanol as **2a**. Yield 64 %.

Preparation of H_2L

The Schiff base was prepared by condensation of the diamine (**2a**) (1 mmol) and salicylaldehyde (2 mmol) over

para-toluene sulfonic acid (*p*-TSA) (10 %) as catalyst with refluxing in the minimum volume of ethanol for 120 min. The mixture was cooled to room temperature and the precipitate filtered off and washed with hot ethanol. Yield 85 %.

Preparation of the free complex

$\text{Cu}(\text{OAc})_2 \cdot 6\text{H}_2\text{O}$ (1 mmol) was dissolved in the minimum of warm ethanol and added to a solution of the Schiff base (1 mmol) in CHCl_3 (20 ml). The mixture was refluxed overnight and then cooled. The product was filtered off, washed with cold water (10 ml) and air-dried. Yield 64 %.

Preparation of copper-exchanged zeolite

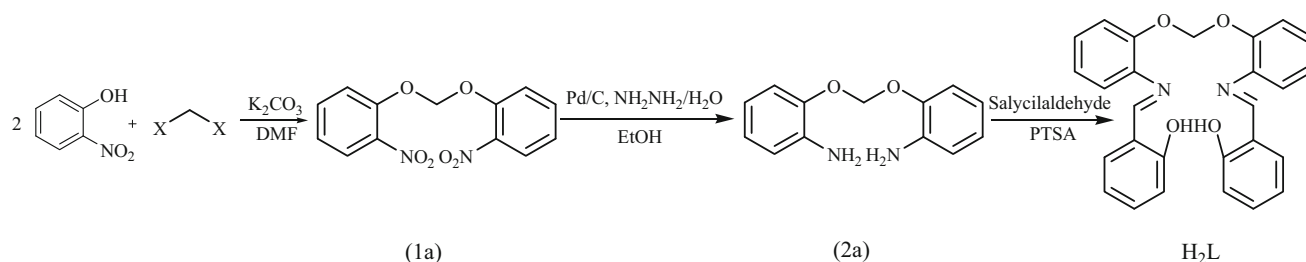
$\text{CuCl}_2 \cdot 2\text{H}_2\text{O}$ (1 mmol) was added to a suspension of zeolite NaY (1 g) in deionized water (100 ml). The mixture was stirred at room temperature for 24 h. The light blue solid was filtered off and air-dried, and then added to a solution of NaCl (200 ml, 0.01 M) and stirred at room temperature for 8 h to remove copper ions from the external surface. Atomic absorption spectroscopy confirmed the absence of copper ions on the surface of the zeolite. This material, designated as Cu(II)/Y, was separated by filtration and dried at 120 °C to constant weight.

Preparation of the encapsulated complex

A mixture of Cu(II)/Y (1.0 g) and H_2L (2.5 g) in chloroform (100 ml) was refluxed for 16 h with stirring. In order to remove the excess ligand, the precipitate was washed with chloroform several times until the washings were colorless. The precipitate was collected and dried at 120 °C, designated as [CuL]-Y.

General procedure for the synthesis of benzimidazoles

In a typical procedure, a mixture containing *o*-phenylenediamine (2.5 mmol), the appropriate aromatic aldehyde (1.25 mmol) and different amounts (0.013, 0.025, 0.05 or



Scheme 1 Synthetic pathway for preparation of the Schiff base

0.075 g) of catalyst (zeolite NaY, Cu(II)/Y, free or encapsulated complexes) was refluxed in 10 ml of solvent (ethanol, acetonitrile, chloroform or DMF) for the required time. On completion of the reaction, as mentioned by TLC, the hot solution was filtered to remove the catalyst, solvent was evaporated, and the residue was recrystallized from ethanol/water (1:2). Spectroscopic data for selected compounds are presented below.

2-Phenyl-1H-benzimidazole (1a): Yield: 89 %; white crystals; FTIR (KBr, cm^{-1}): $\nu = 3344, 3051, 1598, 1462, 1276$; $^1\text{H NMR}$ (acetone- d_6 , 300 MHz): δ (ppm) = 12.00 (br s, 1H), 8.20–8.24 (m, 2H), 7.52–7.63 (m, 5H), 7.19–7.24 (m, 2H); Anal. for $\text{C}_{13}\text{H}_{10}\text{N}_2$: C, 80.4; H, 5.2; N, 14.4 %. Found: C, 80.3; H, 5.4; N, 14.3 %.

2-(4-Nitrophenyl)-1H-benzimidazole (1c): Yield: 87 %; pale red crystals; FTIR (KBr, cm^{-1}): $\nu = 3347, 3025, 1604, 1514, 1342, 1278$; $^1\text{H NMR}$ (DMSO- d_6 , 300 MHz): δ (ppm) = 12.51 (br s, 1H), 7.27–8.42 (m, 8H), Anal. for $\text{C}_{13}\text{H}_9\text{N}_3\text{O}_2$: C, 65.3; H, 3.8; N, 17.6 %. Found: C, 65.3; H, 3.9; N, 17.5 %.

2-(4-Bromophenyl)-1H-benzimidazole (1f): Yield: 87 %; yellow crystals; FTIR (KBr, cm^{-1}): $\nu = 3347, 3054, 1599, 1429, 744$; $^1\text{H NMR}$ (acetone- d_6 , 300 MHz): δ (ppm) = 12.00 (br s, 1H), 8.12 (d; $J = 8.36$ Hz, 2H), 7.70 (d; $J = 8.36$ Hz, 2H), 7.59 (d.d; $J = 5.85$ – 3.14 Hz, 2H), 7.18 (d.d; $J = 5.85$ – 3.14 Hz, 2H). Anal. for $\text{C}_{13}\text{H}_9\text{N}_2\text{Br}$: C, 57.2; H, 3.3; N, 10.3 %. Found: C, 57.1; H, 3.4; N, 10.4 %.

2-(4-Methylphenyl)-1H-benzimidazole (1j): Yield: 90 %; yellow crystals, FTIR (KBr, cm^{-1}): $\nu = 3320, 3063, 1601, 1446, 1286$; $^1\text{H NMR}$ (acetone- d_6 , 300 MHz): δ (ppm) = 12.75 (br s, 1H), 7.27–8.18 (m, 8H), 2.38 (s, 3H); $^{13}\text{C NMR}$ (DMSO- d_6 , 75 MHz): δ (ppm) = 152.9, 142.0, 130.1, 127.9, 126.3, 122.7, 119.1, 111.2, 22.4; Anal. for $\text{C}_{14}\text{H}_{12}\text{N}_2$: C, 80.7; H, 5.8; N, 13.4 %. Found: C, 80.7 H, 5.9; N, 13.4 %.

Results and discussion

Spectroscopic characterization

The FTIR spectra of the free Schiff base ligand, free complex, zeolite NaY and encapsulated complex are illustrated in Fig. 1a–d. Coordination of the ligand is indicated by the presence of a new band at ca. 523 cm^{-1} , assignable to Cu–O stretching vibrations [16]. The spectrum of the free Schiff base exhibited a sharp band at 1282 cm^{-1} assigned to C–O stretching vibrations. Upon complexation, this band was shifted to higher wave number (appearing at 1329 cm^{-1}), supporting coordination of the enolic oxygen atoms to the metal. Furthermore, the FTIR spectrum of the free ligand showed a strong band at 3059 cm^{-1} assigned to intramolecularly hydrogen

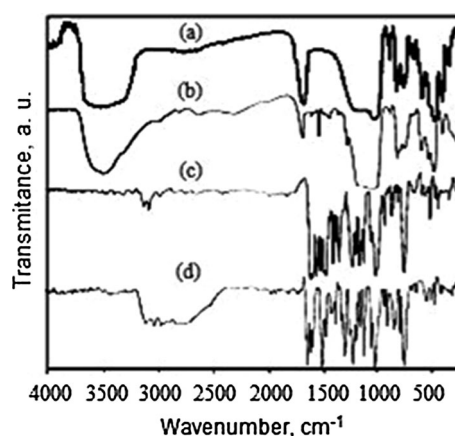


Fig. 1 FTIR spectra of zeolite NaY (a); [CuL]-Y (b); [CuL] (c); H_2L (d) (KBr pellet, sample: KBr 1:6)

bonded O–H groups, which were absent from the spectrum of [CuL]. The C=N stretching vibration was observed at 1618 cm^{-1} as a strong band in the spectrum of the free Schiff base. In the spectrum of [CuL], this band was shifted to lower wave number, appearing at 1587 cm^{-1} which is consistent with binding of azomethine nitrogen atoms to the copper centers [15].

In the FTIR spectrum of the encapsulated complex, bands at 457 and 725 cm^{-1} are attributed to the bending and symmetric stretching vibrations of the Al–O–Si framework, respectively. Asymmetric stretching vibrations of the zeolite Al–O–Si chains are responsible for the strong and broad band at 1026 cm^{-1} , while two absorption bands at 1649 and 3458 cm^{-1} are assigned to lattice water molecules and surface hydroxylic groups [17]. No shift or broadening was observed in the external linkage vibrations (structure sensitive bands: $457, 725$ and 1026 cm^{-1}) upon inclusion of the Schiff base complex, confirming that the zeolite framework remained unchanged, as also indicated by XRD analysis. Encapsulation of the complex is consistent with the observation of bands in the region of 1200 – 1600 cm^{-1} , where the zeolite has no absorptions. The bands related to the complex showed weak intensities, due to its low concentration in the zeolite matrix [17], but their positions were identical to those observed in the spectrum of the free complex. This observation also confirms that the complex retained its structure after the encapsulation and that chemical ligation to the zeolite is either nonexistent or very weak [18]. In the FTIR spectrum of the encapsulated complex, a band at 1584 cm^{-1} was assigned to $\nu_{\text{C=N}}$, while a band at 1321 cm^{-1} was attributed to C–O stretching vibrations. Other bands in region of 1400 – 1600 cm^{-1} can be assigned to C=C stretching vibrations.

The electronic spectra of the free Schiff base and the free complex have been reported previously [15]. The DRS (diffuse reflectance spectrum) of the encapsulated complex

Table 1 Electronic data for the Schiff base and its free and encapsulated complex

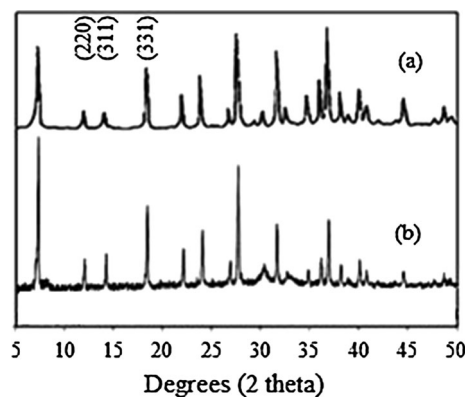
Compound	Wavelength (nm)	Assignment
H ₂ L	255	$\pi \rightarrow \pi^*$ (phenyl)
	345	$\pi \rightarrow \pi^*$ (azomethine)
[CuL]	274	$\pi \rightarrow \pi^*$ (phenyl)
	410	$\pi \rightarrow \pi^*$ (azomethine)
	695	$d \rightarrow d$
[CuL]-Y	269	$\pi \rightarrow \pi^*$ (phenyl)
	405	$\pi \rightarrow \pi^*$ (azomethine)
	683	$d \rightarrow d$

was recorded in Nujol, and the bands are tabulated in Table 1, along with the corresponding data for the free ligand and complex. The Schiff base shows two bands: The first at 255 nm is assigned to phenyl $\pi \rightarrow \pi^*$ transitions, while the second at 345 nm may be attributed to $\pi \rightarrow \pi^*$ transitions of the azomethine chromophores. Both bands are shifted to higher frequencies in the complex, confirming coordination of the imine nitrogen atoms to copper. Ligand-to-metal charge transfer (LMCT) band was also observed, overlapping with the intraligand $\pi \rightarrow \pi^*$ transitions. The free complex also shows weak and broad band at 695 nm and assigned to $d \rightarrow d$ transitions. The DRS spectrum of the encapsulated complex was similar to that of the free complex, consistent with unchanged chemical structure after encapsulation.

X-ray powder diffraction and thermal analysis

Comparison of the X-ray powder diffraction pattern of zeolite NaY with that of the encapsulated complex revealed no new crystalline pattern for the lattice. Hence, the crystallinity of the zeolite is almost intact after inclusion of the complex (Fig. 2a, b) [19]. However, it is clear from the XRD pattern that the line intensity of I_{220} is higher than I_{311} for zeolite NaY, but lower for the encapsulated complex. This difference can be attributed to the presence of the complex within the zeolite supercages. Similar results have been reported in the literature [20].

Figure 3a, b shows TG/DTA curves for zeolite NaY and the encapsulated complex, recorded under a nitrogen atmosphere. The TG/DTA curve of zeolite NaY shows endothermic peaks at 110 and 150 °C related to desorption of physical and chemical water molecules. Four decomposition steps were observed for the encapsulated complex. In the first step, an endothermic weight loss of 9.70 % below 130 °C is assigned to the removal of trapped water. In the second step, there is an endothermic weight loss of 6.62 % in the range of 130–280 °C, related to loss of intrazeolite

**Fig. 2** XRD patterns of zeolite NaY (a) and [CuL]-Y (b)

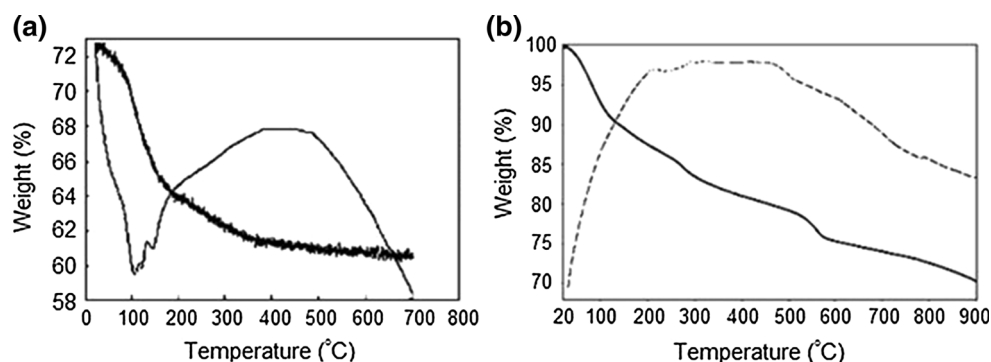
water [21]. The third step involves slow and exothermic decomposition of 8.33 % over a wide range of 280–580 °C due to decomposition of the Schiff base ligand. A disagreement between experimental and theoretical weight loss values was observed in the third step, if we consider the 2.46 % copper content as observed by analytical data (the theoretical value for [CuL]-Y was 16.14 %). This can be explained by the presence of unreacted copper ions in the zeolite void [22]. Finally, the last step with exothermic weight loss of 5.32 % at the range of 585–900 °C is related to changes in the zeolite framework structure.

Analytical data

Analytical data for the parent zeolite NaY, Cu(II)/Y, and the free and encapsulated complexes are given in Table 2. A Si/Al molar ratio of 2.30 for the parent zeolite NaY corresponds to a $\text{Na}_{56}[(\text{AlO}_2)_{56}(\text{SiO}_2)_{136}]$ unit cell formula, while a unit cell formula of $\text{Na}_{37.4}\text{Cu}_{9.7}[(\text{AlO}_2)_{56}(-\text{SiO}_2)_{136}] \cdot n\text{H}_2\text{O}$ is suggested for Cu(II)/Y. No significant change in the Si/Al ratio of Cu(II)/Y and the encapsulated complex was observed, suggesting that no dealumination had occurred during the ion exchange and encapsulation steps. The C/N ratios of the free and encapsulated complexes were also similar, again indicating no change in the structure of the complex after encapsulation. The analytical data for Cu, C, H and N indicated a ligand/metal molar ratio of a little less than unity, due to the inability of the ligand to react with all of the copper within different sites of zeolite NaY [17].

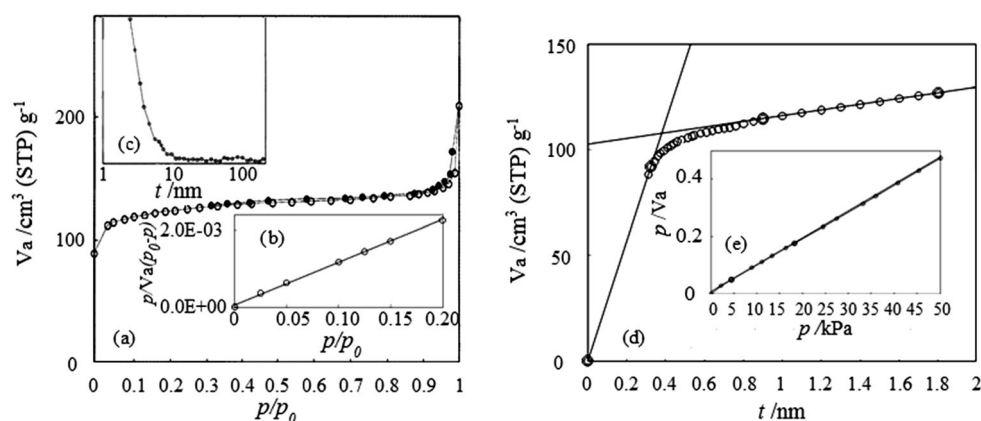
N₂ adsorption–desorption isotherm

The surface characteristics of the encapsulated complex were studied by nitrogen adsorption at 77 K (Fig. 4). Abbo et al. [23] have previously reported the N₂ adsorption–desorption isotherm of pure zeolite NaY. According to IUPAC classification, the isotherms of zeolite NaY and the

Fig. 3 TGA/DTA profiles of zeolite NaY (a) and [CuL]-Y (b)**Table 2** Analytical data for zeolite NaY, Cu(II)/Y, free and encapsulated complexes

Catalyst	Color	% Cu	% C	% N	% H	C/N	% Si	% Al	% Na	Si/Al
Zeolite NaY	White	–	–	–	–	–	20.6	8.9	7.2	2.3
Cu(II)/Y	Bright blue	2.5	–	–	–	–	20.7	9.0	3.7	2.3
[CuL]-Y	Green	2.5	6.4	0.5	0.5	12.8	20.4	8.9	4.8	2.3
[CuL] ^a	Green	12.4	64.7	5.4	3.8	12.0	–	–	–	–

^a The analytical data were reported in Ref. [15]

Fig. 4 N₂ adsorption–desorption isotherm (a), BET plot (b), BJH plot (c), *t*-plot (d) and Langmuir plot (e) of [CuL]-Y

encapsulated complex are type I, whereas according to the Brunauer classification, the isotherm was type III indicating microporous nature of the material [20]. However, the slightly enhanced uptake of N₂ at P/P₀ values greater than 0.9 confirmed the presence of a small quantity of macropores (pores larger than 500 Å). Furthermore, a narrow hysteresis loop was clearly observed for the encapsulated complex which was characteristic of the porous nature of this material (Fig. 4a) [22]. The range of linearization of the BET plot was 0.02–0.2. Also, the catalyst showed a narrow BJH pore size distribution curve as shown in Fig. 4c [23].

BET surface area (S_{BET}), total pore volume (V_p), mean pore diameter derived from the BET plot (D_{BET}) and the BJH plot (D_{BJH}), surface area derived from Langmuir plot (S_{Lang}) and *t*-plot (S_t), micropore volume (V_{mic}), the external surface area of crystals derived from a *t*-plot (S_{ext}) of the encapsulated complex and also BET surface areas

(S_{BET}), total pore volumes (V_p) of zeolite NaY and Cu(II)/Y are listed in Table 3. The surface area and pore volume of the copper-exchanged zeolite showed a negligible reduction in comparison with parent zeolite NaY. However, noticeable reductions in the surface area and pore volume were observed upon encapsulation of the Schiff base complex. Since the FTIR spectrum and XRD pattern confirmed that the crystallinity of the zeolite was retained after the encapsulation, these changes are consistent with the presence of the complexes in the zeolite supercages rather than the external surface. As shown in Table 3, the S_{BET} value of the compound was close to the S_t value, indicating the correct choice of standard *t*-curve [24]. A *t*-plot for this catalyst showed two linear regions. Surface area (S_t) and external surface area (S_{ext}) of the catalyst were obtained by multiplying the slopes of the first and second linear regions, respectively, by 15.47. The *y*-axis intercept of the second line multiplied by the ratio of the gas to

Table 3 Some surface characteristics data of zeolite NaY, Cu(II)/Y and the encapsulated complex

Sample	S_{BET} (m ² /g)	S_t (m ² /g)	S_{Lang} (m ² /g)	S_{ext} (m ² /g)	V_p (cm ³ /g)	V_{mic} (cm ³ /g)	D_{BET} (nm)	D_{BJH} (nm)
NaY	560	n.m	n.m	n.m	0.33	n.m	n.m	n.m
Cu(II)/Y	543	n.m	n.m	n.m	0.31	n.m	n.m	n.m
[CuL]-Y	392	441	468	20.24	0.28	0.17	2.86	2.41

n.m not measured

Table 4 Effect of type and amount of catalyst on the synthesis of 2-phenyl-1H-benzimidazole

Catalyst	Catalyst amount (g)	Time (min)	Yield (%)
–	–	300	Trace
NaY	0.025	300	45
Cu(II)/Y	0.025	120	70
[CuL]-Y	0.025	60	89
[CuL]	0.025	120	59
[CuL]-Y	0.013	90	74
[CuL]-Y	0.05	60	84
[CuL]-Y	0.075	60	77

Reaction conditions: *o*-phenylenediamine (2.5 mmol), benzaldehyde (1.25 mmol), catalyst (0.013, 0.025 and 0.05 and 0.075 g), acetonitrile (10 ml) under reflux conditions

liquid densities of nitrogen (0.00156) provided the micropore volume in cm³/g of solid [25].

Catalytic activity

In order to optimize the reaction conditions for catalysis, the synthesis of 2-phenyl-1H-benzimidazole (**1a**) was chosen as a model reaction. Firstly, the amount of catalyst was optimized. A mixture of *o*-phenylenediamine (2.5 mmol), benzaldehyde (1.25 mmol) and different amounts (0.013, 0.025, 0.05 or 0.075 g) of the required catalyst was refluxed in 10 ml of acetonitrile. As shown in Table 4, zeolite NaY showed a relatively low yield, whereas an increment was observed for Cu(II)/Y. The still higher yield for the encapsulated complex confirms the importance of the ligand in the structure of the catalyst. Furthermore, atomic absorption spectroscopy confirmed that no leaching was observed when the encapsulated complex was used as a catalyst, whereas moderate leaching of copper ions occurred when the reaction was performed over Cu(II)/Y [26]. The encapsulated complex also showed better catalytic efficiency than its free analogue, due to isolation of the copper centers in the former [27]. [CuL]-Y showed the best catalytic activity overall.

As shown in Table 4, the optimum amount of [CuL]-Y was determined as 0.025 g. Higher catalyst loading caused

Table 5 Effect of solvent on the synthesis of 2-phenyl-1H-benzimidazole

Solvent	Time (min)	Yield (%)
MeCN	60	89
DMF	60	84
CHCl ₃	75	67
EtOH	80	52

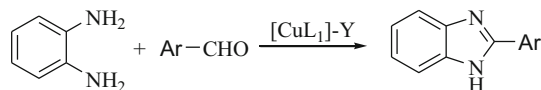
Reaction conditions: *o*-phenylenediamine (2.5 mmol), benzaldehyde (1.25 mmol), [CuL]-Y (0.025 g), solvent (10 ml) under reflux conditions

lower yields, perhaps due to absorption of substrates on the surface of the zeolite [28].

In an effort to improve the yields, various solvents (acetonitrile, DMF, ethanol or chloroform) were screened for the reaction of benzaldehyde (1.25 mmol) with *o*-phenylenediamine (2.5 mmol) in the presence of [CuL]-Y (0.025 g) under reflux conditions (Table 5). Polar solvents such as DMF and acetonitrile proved to be suitable for this reaction, with relatively high yields. In contrast, ethanol showed the lowest yield, perhaps because of its coordination to Lewis acid sites, resulting in a decrease in the catalytic activity [29].

In order to investigate the scope and generality of the encapsulated complex as a heterogeneous catalyst for the synthesis of benzimidazoles, aromatic aldehydes with a wide range of substituents were tested, with the results given in Table 6. Both electron-poor and electron-rich aryl aldehydes afforded good yields.

In order to be sure that the encapsulated complex was responsible for the catalytic effect (rather than copper species leached from the zeolite), 0.025 g of [CuL]-Y was refluxed in 10 ml acetonitrile for up to 24 h and then filtered off. Next, the liquid phase was used as solvent for the synthesis of (**1a**) under the optimized conditions without any added catalyst. Only a trace amount of (**1a**) was obtained, indicating that the catalyst is the encapsulated complex. The absence of leaching during the reaction was also confirmed by atomic absorption spectroscopy and analytical data. Atomic absorption spectroscopy of the final reaction solution confirmed <1 % leaching of copper from

Table 6 [CuL]-Y catalysis of the synthesis of substituted benzimidazole derivatives

Product	Ar	Time (min)	Yield (%)	Melting point (°C) ^a	Ref.:Yield (%)
1a	Phenyl	60	89	284–286	[30]:54
1b	4-Fluorophenyl	65	91	252–254	[30]:39
1c	4-Nitrophenyl	60	87	311–312	[31]:85
1d	4-Methoxyphenyl	70	91	222–224	[32]:75
1e	4-(Dimethylamino)phenyl	80	93	234–236	[32]:72
1f	4-Bromophenyl	65	87	280–282	[30]:80
1g	2-Hydroxyphenyl	60	95	242–244	[30]:29
1h	2-Chlorophenyl	60	88	266–268	[30]:65
1i	4-Chlorophenyl	60	90	285–287	[30]:69
1j	4-Methylphenyl	60	90	279–281	[30]:58
1k	2,4-Dimethoxyphenyl	70	65	253–254	[15]:26
1l	3,4-Dihydroxyphenyl	75	60	258–260	[15]:40

^a Melting point, FTIR and ¹H NMR spectra of products were compared to those reported in the literature

Reaction conditions: *o*-phenylenediamine (2.5 mmol), aldehyde (1.25 mmol), [CuL1]-Y (0.025 g), acetonitrile (10 ml) under reflux conditions

the catalyst. Furthermore, analytical data showed that the copper content of the recycled catalyst had undergone only an insignificant decrease of 0.2 %.

The recyclability of [CuL]-Y was also studied. The synthesis of (**1a**) was performed under the optimized conditions. At the end of the reaction, the catalyst was filtered off, washed several times with acetonitrile, dried at 120 °C and used again under the same conditions. Four consecutive runs gave yields of 89, 85, 79 and 75 %, respectively. Preservation of the crystallinity of the recycled catalyst was also confirmed by its X-ray diffraction pattern. Furthermore, FTIR spectra of fresh and recycled catalyst samples were identical.

Conclusion

A zeolite NaY-encapsulated Cu(II) complex was prepared by the flexible ligand method. The encapsulated complex proved to be an effective catalyst for the synthesis of benzimidazoles. In comparison with parent zeolite NaY, yields of the desired product were increased by using this new catalyst. Furthermore, the encapsulated complex can be recovered and reused without much loss of catalytic activity.

Acknowledgments We gratefully acknowledge the financial support from the Research Council of Arak University.

References

- Sharma S, Gangal S, Rauf A (2009) Eur J Med Chem 44:1751–1757
- Hojati SF, Maleki B, Beykzadeh Z (2011) Monatsh Chem 142:87–91
- Bourissou D, Guerret O, Gabbai FP, Bertrand G (2000) Chem Rev 100:39–92
- Heuser S, Keenan M, Weichert AG (2005) Tetrahedron Lett 46:9001–9004
- Nadaf RN, Siddiqui SA, Daniel T, Lahoti RJ, Srinivasan KV (2004) J Mol Catal A 214:155–160
- Hein DW, Alheim RJ, Leavitt JJ (1957) J Am Chem Soc 79:427–429
- Jenkins GL, Knevel AM, Notes D (1961) J Org Chem 26:274
- Terashima M, Ishii M (1982) Synthesis 6:484–485
- Chkraborti AK, Rudrawar S, Kaur G, Sharma L (2004) Synlett 9:1533–1536
- Hari A, Karan C, Rodrigues WC, Miller BL (2001) J Org Chem 66:991–996
- Clark JH (2002) Acc Chem Res 35:791–797
- Mobinikhaledi A, Foroughifar N, Basaki N (2009) Turk J Chem 33:555–560
- Mobinikhaledi A, Foroughifar N, Zendehtdel M, Jabbarpour M (2008) Synth React Inorg Met Org Nano-Metal Chem 38:390–393
- Breck DW, Tona Wanda NY (1964) Assigned to Union Carbide Pat No. 3,130,007 Patented April 21
- Mobinikhaledi A, Jabbarpour M (2013) Res Chem Intermed. doi:10.1007/s11164-013-1205-1
- Brunel D, Belloccq N, Surta P, Cauvel A, Lasperas M, Moreau P, Drenzo F, Galanequ A, Fajula F (1998) Coord Chem Rev 178:1085–1108
- Zendehtdel M, Khanmohamadi H, Mokhtari M (2010) J Chin Chem Soc 57:205–212

18. Salavati-Niasari M, Shaterian M, Ganjali MR, Norouzi P (2007) *J Mol Catal A-Chem* 261:147–155
19. Slavati-Niasari M, Salimi Z, Bazarganipour M, Davar F (2009) *Inorg Chim Acta* 362:3715–3724
20. Maurya MR, Kumar M, Titinchi SJ, Abbo HS, Chand S (2003) *Catal Lett* 86:97–105
21. Maurya MR, Chandrakar AK, Chand S (2007) *J Mol Catal A-Chem* 270:225–235
22. Chatterjee D, Mitra A (1999) *J Mol Catal A-Chem* 144:363–367
23. Abbo HS, Titinchi SJ (2010) *Top Catal* 53:1401–1410
24. Thabet MS, Ahmed AH (2013) *J Porous Mater* 20:319–330
25. Gregg SJ, Sing KS (1982) *Adsorption, surface area and porosity*. Academic Press, New York
26. Salavati-Niasari M (2009) *J Incl Phenom Macrocycl Chem* 65:349–360
27. Naeimi H, Moradian M (2013) *Appl Catal A-Gen* 467:400–406
28. Massa PA, Ayude MA, Fenglio AJ, Gonzalez JF, Haure PM (2004) *Lat Am Appl Res* 34:133–140
29. Mobinikhaledi A, Zendejdel M, Safari P (2013) *React Kinet Mech Cat*. doi:10.1007/s11144-013-0609-7
30. Grimmett R (1997) *Imidazole and benzimidazole synthesis*. Otago University, Academic Press, New York
31. Shingalapur RV, Hosamani KM (2010) *Catal Lett* 137:63–68
32. Han X, Ma H, Wang Y (2008) *Russ J Org Chem* 44:863–865